The impact of host heterogeneity on pathogen evolution depends on spatial structure

Elisa Visher[1,2], Anisha Ali[3,4], Jonathan Barajas[3], Sehar Masud[3], Annika McBride[3], Edwin Ramos[3], Melissa Sui[3,5], Cristina Villalobos-Heredia[3], Natalie Walzer[3], P. Signe White[1], Mike Boots[1,6]

1 Department of Integrative Biology, University of California, Berkeley, CA, 94720, USA

2 Department of Genetics, Stanford University, Stanford, CA, 94305, USA

3 University of California, Berkeley, CA, 94720, USA

4 Department of Psychology, Cal State East Bay, CA, 94542, USA

5 Department of Plant and Microbial Biology, University of California, Berkeley, CA, 94720, USA

6 5 College of Life and Environmental Sciences, University of Exeter, Penryn Campus, Penryn, TR10 9FE, UK

ABSTRACT

Host diversity and spatial structure both separately impact parasite evolution and may also interact when space structures host heterogeneity and populations must adapt to both selection pressures. Here, we experimentally evolve granulosis virus in microcosms of its *Plodia interpunctella* (Indian meal moth) host that vary in spatial structure and host genetic diversity. We do this by manipulating food viscosity (spatial structure) and adding either one (homogeneous) or two (heterogeneous) host genotypes to the microcosm. Spatial structure therefore bot generally structures of infectious contacts and decreases the rate of contact between genotypes. We preserve spatial structure across passages and assay virus from different positions on the two host genotypes. We find that virus evolves specific interactions with its locally familiar host genotype, but that the impact of specialization on evolved phenotypes depends on the spatial structure. In spatially structured treatments, exploitation rates are higher on the familiar host, while, in well-mixed treatments, they are lower. We also find that virus can specialize to their locally familiar host in heterogeneous microcosms when spatial structure lowers contact rates between hosts. These results demonstrate that host genetic diversity and spatial structure can interact to reshape the evolution of pathogen host range. [197/200]

INTRODUCTION

A body of literature on the 'monoculture effect' has shown that host genetic diversity affects infectious disease dynamics in both ecological and evolutionary contexts [1–5]. Specifically, genetically diverse host populations can decrease the prevalence of infectious diseases and may constrain their evolution of transmissibility or virulence [3,6–12]. This can be explained by heterogeneous host populations limiting the transmission of specialist pathogens and thereby selecting for 'mediocre' generalists that may be constrained by costs associated with trade-offs or with the lesser evolvability of generalists [13–19].

This theory, however, considers scenarios where the genetic diversity of the host population is well-mixed so that transmission occurs readily between host types. However, it is clear that many host populations exhibit some sort of spatial or contact network structuring. In this case, a parasite lineage may be more likely to infect one host type even if the population is genetically diverse overall. Several theoretical studies have examined this scenario by manipulating the contact matrix between hosts to show that the degree of mixing in a population should change the evolutionarily optimal strategy for host range [20–22]. Higher contact rates between host types should select for generalists [20–22], but some models show that it can also lead to greater specialization when migration increases the amount of genetic variation that selection can act upon and increases local competition for patches [23–25]. Additionally, spatially structured transmission is, by itself, also predicted to affect parasite evolution because 'self-shading' should select for less infective, more prudent pathogens [26–34]. However, some theory suggests that there may be regions of parameter space where intermediate levels of spatial structure select for more exploitative pathogens [28,33]. Current host mixing models do not explicitly consider these effects of spatial structure within their frameworks and there may be additional ways that host range and life history trade-offs interact if we consider that it may easier to become a generalist if 'mediocre', intermediate phenotypes are already optimal [35]. Therefore, there are open questions for how we expect spatial structure and host genetic diversity to interact, both in terms of how host type mixing affects host range evolution and also in terms of how these different selection pressures interact.

We explore these interactions by experimentally evolving granulosis virus in microcosms of its *Plodia interpunctella*, or Indian meal moth (Hübner), host that vary in their host genetic diversity and spatial structuring. We manipulate spatial structure by altering the viscosity of the food medium that larvae live within [30,36,37], and we alter host heterogeneity by adding larvae from either the same or different inbred populations (host genotypes) to either half of the microcosm [38] (Figure 1). The treatments are then fully crossed so that each host treatment is in both food viscosity treatments. Altering host genetic diversity allows us to examine the consequences of host heterogeneity on virus evolution [6,7,10,16], while altering the spatial structure of micocosms manipulates the contact rates between hosts and structures infectious contacts [20,30]. Our experiment therefore explores how spatial structure and host heterogeneity interact and how the spatial structuring of heterogeneity affects its impact on pathogen evolution.

We find that manipulating the spatial structure of a population can change the impact of specialization on pathogen phenotypes in that virus populations reverse whether they have lower or higher exploitation metrics on their familiar host than on the foreign host depending on the spatial structure of their evolution condition. We also find that virus in heterogeneous microcosms is more locally specialized when there are lower migration rates between the host types. These results suggest that interactions between selection pressures may result in idiosyncratic patterns of parasite specialization when parasites are simultaneously optimizing life history trade-offs and host range. Furthermore, these results suggest that heterogeneous host populations may support assemblages of specialized parasites when spatial structure decreases contact rates between host types. This work therefore has implications for our theories about how host diversity affects infectious disease evolution and control, and, more generally, for how interactions between selection pressures can lead to evolutionary outcomes unexpected by theory based on individual trade-offs [35,39,40].

METHODS

Study system

Plodia interpunctella, or the Indian meal moth, is a stored grain pest that naturally lives at high population density within its cereal food medium for 5 larval instar stages before it pupates into an adult moth that disperses, mates, and lays eggs, but does not eat [41,42]. It is naturally infected by the *Plodia interpunctella* granulosis virus (PiGV), a dsDNA baculovirus that transmits when larvae directly cannibalize infection killed cadavers or consume virus that was released into the environment from such cadavers [43,44]. Thus, the virus is an obligate killer that will only transmit if it kills its host. Notably, the virus can only infect *P. interpunctella* during the larval stages and, if exposed larvae clear the infection, they can pupate and carry out the rest of their life history as normal [45]. Infection killed cadavers are recognizable because successful infection turns larvae an opaque, chalky white color due to the high density of viral occlusion bodies [46]. The system has proved a powerful tool for examining the effects of spatial structure on pathogen exploitation rates and, more recently, host genotype specialization [30,38].

Host genotype selection and maintenance

For this experiment, we selected two inbred populations of *P. interpunctella* that were previously generated in the lab by brother-sister mating individuals for >27 generations [47]. Each population should therefore be essentially a clonal population of two distinct host genotypes (Genotype 9 and Genotype 17). These genotypes were chosen because they had similar levels of general resistance or, alternatively worded, the ancestral virus has similar levels of initial infectivity on them [38] (Table S2, Figure S3). We have previously shown that virus evolved in homogeneous populations of these specific host genotypes can specialize on its familiar host genotype by increasing their infectivity and/or productivity [38].

We maintained these genotypes as inbred lines in wide-mouthed Nalgene pots (ThermoFisher Scientific, U.K.) in the absence of infection with 200g 'Standard' food medium (made in batches of 500g cereal mix (50% Earth's Best oatmeal, 30% wheat bran, 20% rice flour), 100g brewer's

yeast, 2.2g sorbic acid, 2.2g methyl paraben, 125ml honey, and 125ml glycerol) in incubators set at 27±2 °C and 35±5% humidity, with 16:8hr light: dark cycles [48]. To maintain populations, ~50 adult moths were moved into a new pot with new food when they emerged monthly. Thus, host lines were maintained in the absence of infection and did not evolve throughout the experiment.

Manipulating spatial structure

We manipulated spatial structure in the experiment by changing the viscosity of the food medium as in [30,36,37]. Because larvae live within their food medium, this alters individuals' dispersal patterns and thus the spatial structure of their infectious contacts. We made food of two viscosities, 'loose' and 'sticky', which differ solely in the amount of glycerol added. 'Loose' food contains 500g Earth's Best oatmeal, 100g brewer's yeast, 2.2g sorbic acid, 2.2g methyl paraben, and 175ml glycerol. 'Sticky' food contains 500g Earth's Best oatmeal, 100g brewer's yeast, 2.2g sorbic acid, 2.2g methyl paraben, and 450ml glycerol. 'Loose' and 'sticky' food was then added to wide-mouthed Nalgene pots and frozen overnight to kill any insect eggs potentially contaminating the food. The mass of food added to these pots (300g 'loose' and 550g 'sticky' food) was determined by the volume needed to entirely fill half of one of our plastic microcosm containers. We tested the impact of food viscosity on spatial structure in several ways. First, we measured life history traits (development time and mass at pupation) of larvae added to assay grids with 'sticky' and 'loose' food (as in [48]) to ensure that food viscosity did not affect these metrics (Figure S1). Second, we added 'loose' and 'sticky' food to 4 cm diameter PVC pipes (10 each), added 11-day old 3rd instar larvae to one side of the pipe, and measured how far larvae dispersed after 10 days (Table S1). Finally, we set up microcosms with the two food types as in our experiment below but added food containing larvae to only one half of the microcosm and sterile food to the other half. We incubated these microcosms for 21 days, then recorded the position of every individual (Figure 2C).

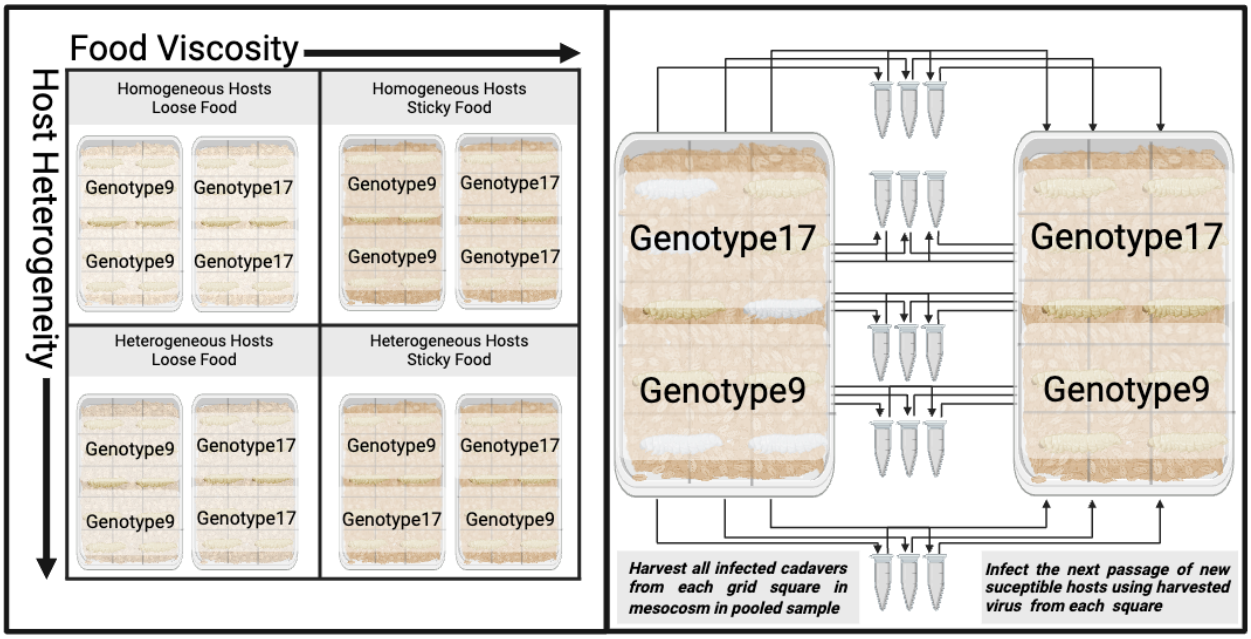

Figure 1: Experimental design and passaging scheme. (Left) Each microcosm was set up by adding 2 pots of food containing 11-day old larvae to opposite vertical ends of a plastic microcosm with a 3x5 grid. The 3rd row of the grid is therefore a contact zone between the hosts. There are 3 replicates for each of the 8 microcosms. There are 4 different treatment types of homogeneous or heterogeneous hosts by 'loose' or 'sticky' food. Each homogeneous treatment was set up with both host types and each heterogeneous host treatment was set up alternating which host was on 'top' or 'bottom' of the grid. Microcosms were consistently oriented in the growth chamber so that the 'bottom' side was closer to the door. (Right) After 20 days incubating with virus, microcosms were frozen and dissected into grid squares. All infected larvae from each grid square were harvested, added to a 1.5mL Eppendorf tube (1 square per tube), and homogenized to release occlusion bodies. 500mL of the virus solution was then pipetted in droplets over the same grid square of a new microcosm of the same treatment set-up with fresh 11-day old hosts. Therefore, the spatial force of infection was preserved across passages. We experimentally evolved virus for 10 passages.

<u>Setting up host populations for microcosms</u>

After thawing the pots of 'sticky' and 'loose' food, we added ~50 similarly aged adult moths to each pot from either our Genotype 9 or Genotype 17 host maintenance populations and incubated them for 10 days. These single-genotype adults mated and laid eggs into the 'sticky' or 'loose' food. 10 days after adding adults, these pots were used to set up microcosms as in Figure 1. While pots were set up with the same number of adults, they may not have contained the same number of larvae. Observationally, population sizes may have varied from a couple dozen individuals to mid-hundreds of individuals.

Microcosms were set up in 9.25" x 12.08" x 0.9" inch plastic A4 document cases (Daiso Japan, U.S.A.) that had been marked with an even 3 x 5 grid of 3.08" x 2.42" squares. We set up 8 microcosms per replicate: 1) homogeneous Genotype 9 hosts in 'loose' food; 2) homogeneous Genotype 17 hosts in 'loose' food; 3) homogeneous Genotype 9 hosts in 'sticky' food; 4) homogeneous Genotype 17 hosts in 'sticky' food; 5) heterogeneous hosts (Genotype 9 on top / Genotype 17 on bottom) in 'loose' food; 6) heterogeneous hosts (Genotype 17 on top / Genotype 9 on bottom) in 'loose' food; 7) heterogeneous hosts (Genotype 17 on top / Genotype 9 on

170 bottom) in 'sticky' food ; and 8) 7) heterogeneous hosts (Genotype 9 on top / Genotype 17 on
171 bottom) in 'sticky' food (Figure 1). Each microcosm therefore had a single food type (either
172 'sticky' or 'loose'), according to its treatment. To arrange hosts in the microcosm, we added 2
173 pots of the food containing 10-day old larvae to opposite vertical ends of the grid, so that food
174 fully filled the plastic containers. For homogeneous host treatments, we added 2 pots containing
175 larvae of the same genotype and, for heterogeneous treatments, these 2 pots contained larvae
176 of different genotypes. Thus, homogeneous genotype microcosms had a single genotype of host
177 throughout the grid, while heterogeneous microcosms had two genotypes separated vertically
178 across the grid with a contact zone at the 3rd row. To balance our treatments and account for
179 potential effects due to position within the grid, we set up 2 microcosms of each of the 2
180 heterogeneous treatments and alternated which genotype is on 'top'.

181 These microcosms were then incubated overnight, as above, so that virus could be added to them
182 on day 11. We repeated this process each passage to set up new microcosms so that evolving
183 virus were added to a fresh microcosm. This allowed us to maintain 2 non-interbreeding and non-
184 evolving host genotypes in our microcosms and preserve the spatial structuring of such
185 genotypes across passages.

186 Experimental evolution

187 We set up 3 replicates of each of our 8 unique microcosm types (24 serially passaged microcosms
188 total). We initiated serial passage by pipetting 5ml of 10^{-2} stock virus solution in small droplets
189 evenly over the top of each microcosm. Each microcosm was then incubated for 20 days and then
190 frozen overnight to kill larvae for harvesting. Passage lengths (10 days before set-up, 1 day
191 overnight, 20 days with virus) therefore roughly correspond to the host's natural ~monthly
192 cyclical demography [37]. We stagger the replicates' passaging schedules weekly due to the time
193 intensive nature of passaging.

194 To harvest virus, we dissected each microcosm by grid square and separately collected infection
195 killed cadavers from each square in sterile 1.5ml Eppendorf tubes (Figure 1). We added 1ml
196 sterile, MilliQ water to each square's tube and used a sterile pellet pestle (Fisher Scientific, U.S.A.)
197 to manually burst larvae and release viral occlusion bodies. We dropleted 500ul of this solution
198 from each square onto the same square of that treatment's freshly set-up microcosm to infect
199 the next passage and froze the rest of the solution. Therefore, we preserved the force of and
200 spatial structure of infection within the grid across passages. We recorded the number of infected
201 cadavers in each square at each passage to track the spatial ecology of infection in the
202 experiment.

203 The microcosms newly infected with passaged virus were then placed back into incubators for 20
204 days to allow the virus to infect larvae for the next passage. We experimentally evolved virus for
205 10 passages, a number standard for microbial evolution experiments. There were several
206 occasions where we had to use the frozen virus solutions reserved during passaging to re-set up
207 passages due to low numbers of infected cadavers or contamination with another pathogen. Low
208 infected numbers were caused by low total population sizes and tended to happen in batches
209 when a set of adults did not breed for whatever reason. There were no observable trends in when
210 this would occur. Bt contamination was much rarer and also tended to happen in batches
211 (potentially when a food batch had been contaminated) without observable trends.

212 Contamination was recognizable because the most common contaminant, *Bacillus thuringiensis*
213 (Bt), turns infected larvae black rather than white [49]. We could generally expect any co-infected
214 larvae to display the black phenotype since Bt kills larvae more quickly (Yitbarak, unpublished
215 data), so re-setting up passages when Bt was visually detected would clear the virus population
216 and prevent co-infection from selecting on evolving virus. Congruously, we did not see any signs
217 of persistent contamination within our passages nor in any of our assays.

218 Assay

219 After passage 10, we collected virus infected cadavers from each square as above. We next
220 pooled the virus from the 3 squares in each row of the 3x5 grid in equal proportion so that we
221 had 5 virus samples per microcosm. Each pooled sample was therefore the virus population at a
222 certain vertical position within the microcosm, along the gradient of heterogeneity for the
223 heterogeneous host microcosms. We purified virus by centrifuging for 1 min at 3000 rpm to
224 remove larger particulate matter and then 3 min at 13000 rpm to pellet virus. We ran these
225 samples through a .65 micron filter to semi-purify our virus of larger bacterial and fungal
226 contaminants, as in [38]. Next, we quantified the concentrations of each sample by counting
227 occlusion bodies on a Petroff-Hauser counting chamber with 400x darkfield microscopy and
228 diluted each to an assay dose concentration of ~7.5x10^8 occlusion bodies per mL in 2% sucrose
229 and .2% dye [38]. The sugar entices the larvae to ingest the virus and the dye allows the
230 experimenter to determine which have ingested half their body lengths of solution and are
231 considered exposed.

232 We assayed each pooled virus sample on both of our 2 host genotypes, Genotype 9 and Genotype
233 17, in a balanced, batched design (see Table S3) to determine the proportion of hosts each virus
234 sample infects on each genotype and the average number of occlusion bodies each virus sample
235 produces per infection on each genotype. With 5 virus samples for each of the 8 microcosms that
236 have 3 replicates, this resulted in 240 virus sample x assay genotype combinations. Because only
237 1 genotype is assayed per day and there are strong day effects within the system, we included
238 assay genotype and set-up date in all statistical models to account both for any general
239 differences in resistance and assay day effects. Furthermore, conclusions are drawn from
240 comparing the relative phenotypes of evolved virus on the different assay genotypes rather than
241 comparing to the ancestral population that was assayed separately (Figure S3, Table S2).

242 To set up infectivity assays, we first moved ~70-80 adult moths of the appropriate host genotype
243 into new pots with 200g 'standard' food. Eleven days after setting up assay pots, we collected
244 100 third instar larvae for each assay combination in a petri dish and starved them under a damp
245 paper towel for 2 hours. After starvation, we syringed tiny droplets of the appropriate virus-
246 sucrose-dye solution onto the petri dish for the larvae to consume. We added 50 larvae that have
247 orally ingested half their body lengths of virus solution to 2 25-cell compartmentalized square
248 petri dishes (ThermoFisher Scientific, U.S.A.) with 'standard' food and incubated them for 20 days
249 [38]. Assay grids were labelled with random identifiers to blind assay combinations and prevent
250 bias. After 20 days, assay grids were frozen and destructively sampled to count the number of
251 infected and uninfected individuals. Infected cadavers from each assay grid were then saved in a
252 pooled sample for virus quantification.

253 To determine the average number of occlusion bodies produced per infected individual, we
254 extracted virus from the pooled samples from each assay grid using a sterile pellet pestle (Fisher
255 Scientific, U.S.A.) to manually burst larvae and release viral occlusion bodies. We then centrifuged
256 these samples as above, but did not filter them, and counted occlusion bodies on a Petroff-
257 Hauser counting chamber. The concentration of occlusion bodies was then divided by the
258 number of infected cadavers that were in the pooled sample to get the average number of
259 occlusion bodies produced per infection for each virus sample on each host genotype.

260 Statistical analyses

261 We analyzed our data using a generalized linear mixed modelling framework in R [50]. All models
262 were run in R version 4.2.3 (2023-03-15) -- "Shortstop Beagle" [51]. We used packages
263 'glmmTMB' and 'lme4' to build models, 'DHARMa' to check model residuals, 'afex' and 'car' to
264 determine significant model terms, 'emmeans' to extract effects, 'tidyverse' to manipulate data,
265 and 'patchwork' and 'ggplot2' to plot results [52–60]. We determined error structures for models
266 by testing fitted models with 'DHARMa' and then adjusting to best fit residuals. On occasion,
267 observation level random effects were used to correct overdispersion in our models [61]. Where
268 necessary, contrasts were used with 'emmeans' to determine effect estimates for treatments.
269 All model tables and annotated code are in the supplement. Models are named in the table (MS,
270 M1-6) and referenced in the manuscript as appropriate.

271 Spatial structure analysis

272 First, we analyzed how larvae moved in our microcosm food viscosity test (Figure 2A) by asking
273 whether the total count of individuals in a square is predicted by an interaction between the
274 viscosity of the food and the distance (in square number) that the square is from where larvae
275 were added (with squares where larvae were directedly added coded as 0) (MS2). The model
276 uses a poisson error structure with observation level random effects. We next examined how
277 food viscosity spatially structured infection during the evolution experiment using the data
278 collected on the number of infected individuals in each square at each passage for each
279 microcosm. To do this, we ran a Levene's Test for Homogeneity of Variance on the infected count
280 data to determine if our 'sticky' and 'loose' food treatments differ in their variance, a measure of
281 how 'clumpy' infection is within a microcosm (MS1).

282 Assay analysis

283 Infectivity and productivity assay data were analyzed in a generalized linear mixed modeling
284 framework using the same packages and process as above [50]. We built models treating
285 proportion infected, average number of occlusion bodies per infected individual, and the
286 composite exploitation rate (proportion infected multiplied by the average virus count) as our
287 response variables. We transformed average virus counts and composite exploitation rates by
288 multiplying and rounding them to produce integer counts for Poisson and negative binomial
289 distribution assumptions. In each model, we included random effects for batch and the nested
290 effect of virus sample under replicate under treatment.

291 First, we asked whether there are significant interaction effects between the genotype that the
292 virus is being assayed on, the host treatment that the virus is from, and the spatial structure that
293 the virus is from by building models with a three-way interaction between these terms (M1). To

more closely look for trends in our data, we asked whether virus populations significantly differ in their specialization at the whole microcosm level by building models that include an interaction effect between the assay being on the host that the population was evolved on ('familiar') or the foreign host and the type of food the population evolved in (M2). Virus from heterogeneous populations was coded as 'heterogeneous' as they do not have a familiar or foreign host at the whole microcosm level. We also included assay genotype as a fixed effect to account for any overall differences in resistance between our assay host genotypes. Model convergence issues prevented us from including the evolution genotype in all models, but, since this term had very weak effects ($p>0.9$) in the models that did converge, we dropped the term to improve comparability across models. The infectivity model uses a binomial error structure with observation level random effects, the productivity model uses a Poisson error structure with observation level random effects, and the exploitation rate model uses a zero-inflated negative binomial error structure with observation level random effects. To better see the effects of specialization in the homogeneous populations, we also ran these same models for the homogeneous host treatments only with the infectivity model using a binomial error structure, the productivity model using a Poisson error structure, and the exploitation rate model using a negative binomial error structure with observation level random effects (M3).

Next, we asked whether spatial structure or host heterogeneity have significant effects on viral phenotypes across genotypes (without accounting an effect of specialization). We built models for infectivity, productivity, and composite exploitation with the same random effects as above, and without fixed effects for being assayed on the familiar or foreign host. For host heterogeneity models, we included the assay genotype, food type, and whether the treatment had homogeneous or heterogeneous hosts as fixed effects, allowing for an interaction between food type and treatment heterogeneity (M4). The infectivity model uses a binomial error structure with observation level random effects and the productivity and composite exploitation models use a zero-inflated negative binomial error structure with observation level random effects. For spatial structure models, we include the food type and assay genotype as fixed effects with the same random effects as above (M5). The infectivity model uses a binomial error structure, and the productivity and composite exploitation models use a zero inflated negative binomial structure with observation level random effects.

Finally, we asked whether virus phenotypes are spatially structured within the heterogeneous host treatments (M6). First, the local proportion of host genotypes during evolution was determined for each virus population by its distance from the host contact zone so that the edge of the microcosm where host genotype 17 was added was coded as 1, the next row of the grid was coded .75, the middle contact zone was coded as 0.5, the following row was coded as .25, and the edge of the microcosm where host genotype 9 was added was coded as 0. Thus, the inverse represents the local proportion of host genotype 9. We built models for infectivity, productivity, and exploitation rate that included the local proportion of host genotype, the host genotype of the assay, the food type, an interaction effects between these three terms, and the order of genotypes in the microcosm as fixed effects. We included the same random effects as in the previous models for batch and nestedness and also for the specific position. The infectivity model uses a binomial error structure, the productivity model uses a Poisson error structure with

observation level random effects, and the exploitation rate model uses a zero-inflated negative binomial error structure.

RESULTS

Food viscosity spatially structures infection

In our experiments testing how food viscosity affected larval movement, we see that 'sticky' food greatly decreases larval dispersal (Figure 1A, Table S1). In microcosms where larvae are only added to one side, the count of individuals found in a grid square after 21 days is significantly affected by the interaction between the distance that the square is from where larvae were added and the food viscosity (MS2 ANOVA $p < 0.001$), with larvae in sticky food dispersing less (MS2 GLMM effect estimate = -3.8, $p < 0.001$). Interestingly, neither the effect of distance ($p = 0.96$) nor food viscosity ($p = 0.07$) significantly affects the count in a grid square alone (MS2 ANOVA). Across the evolution experiment, treatments with different food viscosities differ in the variance of their infected count data ($p < 0.001$, MS1), with 'sticky' food having more clustered infected individuals (Figure 2B).

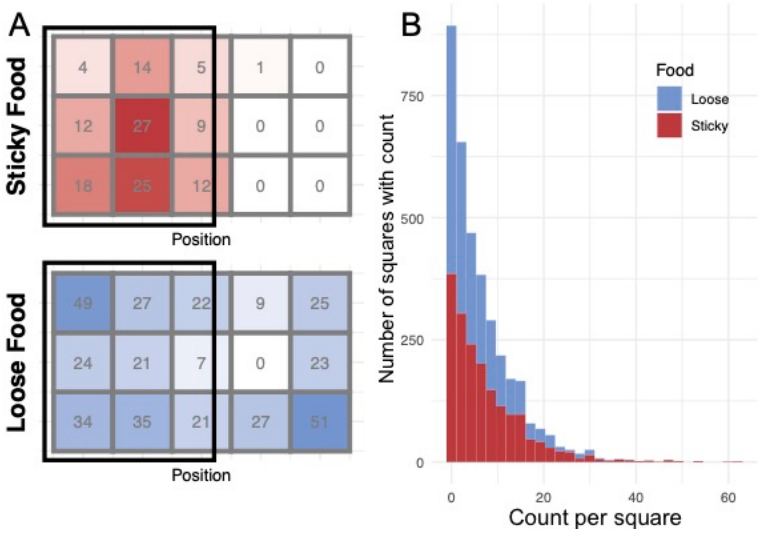

Figure 2: (A) Heatmaps of where individuals are found after 21 days in test microcosms of 'sticky' (top) and 'loose' (bottom) food where food containing larvae has been added to one half of the microcosm (black box) and sterile food to the other. Numbers represent the total number of individuals found in each square. (B) Histogram showing the number of grid squares (y-axis) with different counts of infected larvae (x-axis) during serial passage. Variance is higher in the 'sticky' food condition (MS1).

The impact of specialization on virus phenotypes depends on spatial structure

Averaged across host genotypes, the spatial structure manipulation does not affect virus populations evolved per particle infectivity (M5i ANOVA $p = 0.96$) or per infection virus productivity (M5p ANOVA $p = 0.58$) (Figure S5). This is in contrast to previous results that only assay virus on familiar, genetically diverse hosts [30]. However, any impact of spatial structure may also depend specialization as evolved virus populations are assayed on both familiar and

364 foreign hosts. When we test whether spatial structure interacts with host genotype
365 specialization, we find that there are interactions between which host genotype the population
366 was evolved on, the host genotype assayed on, and the type of food evolved on (M1) (Figure S3,
367 Figure S4). Specifically, for virus populations evolved in homogeneous host populations, the
368 effects of food type (M3i ANOVA p = 0.725), assay genotype (M3i ANOVA p = 0.18), Self (M3i
369 ANOVA p = 0.059), and the Self:Food interaction (M3i ANOVA p = 0.082) are not significant to the
370 model. Viruses from 'loose' food populations are less infective on their familiar host (M3i
371 contrasts effect estimate = -0.785, p = 0.031) while those from 'sticky' food populations do not
372 significantly differ in infectivity between familiar and foreign hosts (M3i contrasts effect estimate
373 = 0.442, p = 0.22) (Figure 3B). For productivity, the effects of food type (M3p ANOVA p = 0.59),
374 assay genotype (M3p ANOVA p = 0.38), Self (M3p ANOVA p = 0.03, GLMM effect estimate Foreign
375 = 1.29 , p = 0.037), and the Self:Food interaction (M3p ANOVA p = 0.12) vary in significance to
376 the model. Viruses from 'loose' food populations are less productive on their familiar host (M3p
377 contrasts effect estimate = -0.451, p =.032) while those from 'sticky' food are significantly more
378 productive on familiar hosts (M3p contrasts effect estimate = 0.198, p =0.347) (Figure 3D).
379 Collectively, for composite exploitation rate, the effects of food type (M3c ANOVA p = 0.08), assay
380 genotype (M3c ANOVA p = 0.98), Self (M3c ANOVA p = 0.037, GLMM effect estimate Foreign =
381 0.45, p = 0.03), and the Self:Food interaction (M3c ANOVA p = 0.047, GLMM effect estimate
382 Foreign:Sticky = -2.31 , p = 0.047) vary in significance to the model. Importantly, the effect of
383 being assayed on a familiar or foreign host depends on food type so that the viruses are more
384 prudent on their familiar hosts in 'loose' food and more exploitative on familiar hosts in 'sticky'
385 food (M3c contrasts loose effect estimate=-1.29 p=0.037; sticky effect estimate=1.02, p=0.09)
386 (Figure 3F).

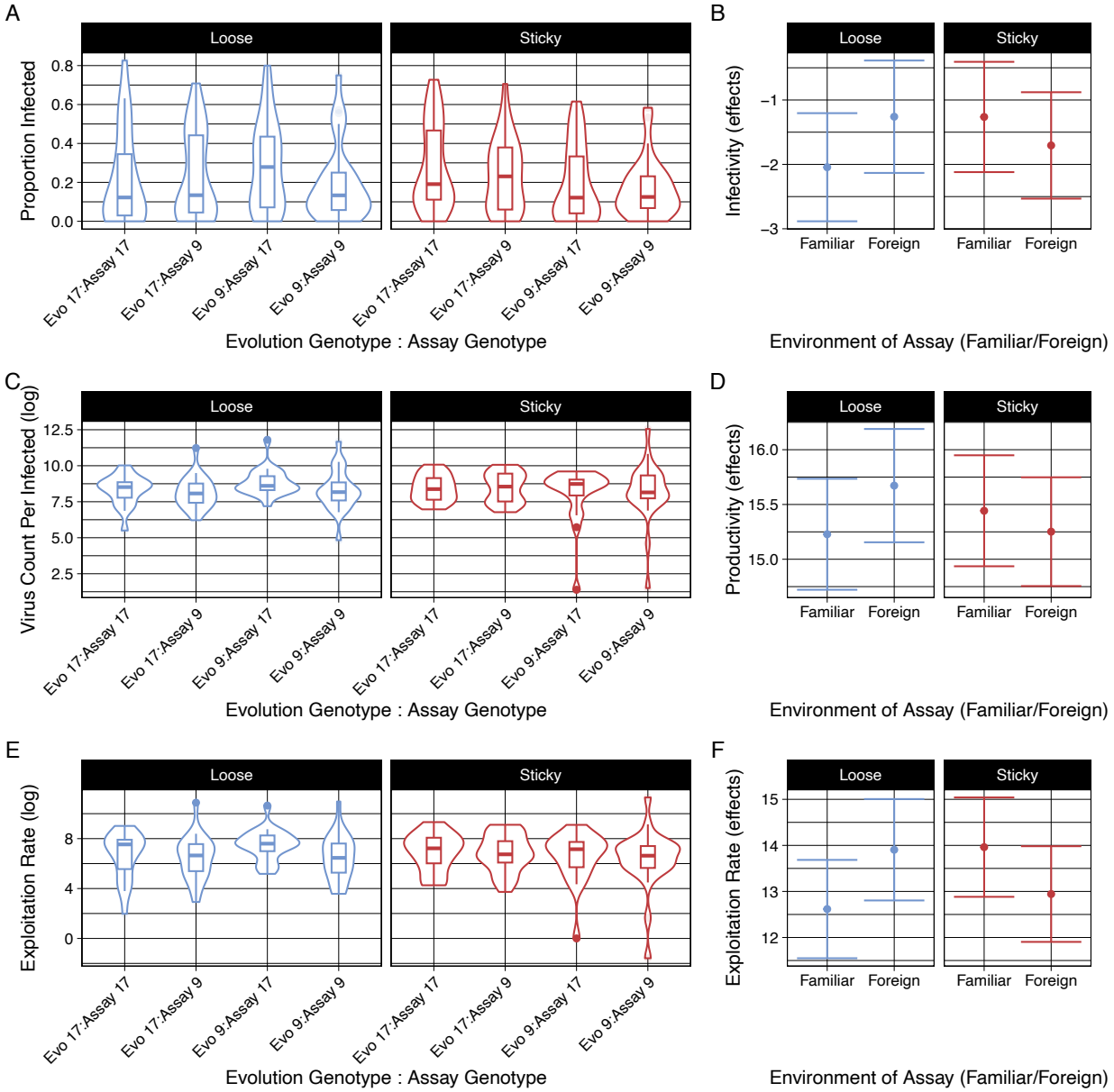

*Figure 3: Interactions between specialization and the spatial structuring of infection in homogeneous microcosms. Panels A, C, E plot raw data and panels B, D, F show model effect estimates drawn from M3 GLMMs. Y-axes represent: (A) proportion infected, (B) effect estimates for the M3i infectivity model, (C) average number of occlusion bodies produced per infectious cadaver on a log scale, (D) effect estimates for the M3p viral productivity model, (E) composite exploitation rate (proportion infected * average number of occlusion bodies) on a log scale, and (F) effect estimates for the M3c exploitation rate model. A, C, E X-axes represent the combinations of which host genotype the virus population evolved on and which they were assayed on. B, D, F X-axes represent whether the virus was being assayed on the host genotype that it evolved on (familiar) or on the foreign host genotype. Panels show whether the virus came from a treatment with 'loose' food or 'sticky' food.*

Spatially structured host genetic diversity leads to local specialization

On average, virus populations evolved in heterogeneous host populations do not significantly differ in infectivity (M4i ANOVA, p = 0.60) or composite exploitation (M4c ANOVA, p=0.20) from those evolved in homogeneous host populations and are slightly more productive (M4p GLMM effect estimate = 0.15, p = 0.04). However, heterogeneous host populations have gradients of host mixing within them as the different positions are different distances from the other host genotype. Additionally, we expect spatial structure to impede host movement and thus further alter the degree of host mixing for different positions. Therefore, we explore whether there is an effect of host specialization within the heterogeneous host microcosms and whether this effect is altered by the spatial structuring of the population. We find that, for composite exploitation rate, there is a significant interaction between the local proportion of a host genotype during evolution (i.e. the position's distance from the contact zone), the assay host genotype, and the type of food evolved in (M6c ANOVA p = 0.031, Figure 4). As in homogeneous populations, virus populations are biased towards higher exploitation rates on familiar hosts in 'sticky' food populations (M6c pairwise contrasts effect estimate = 1.7, p = 0.03) and somewhat lower exploitation rates on familiar hosts in 'loose' food populations (M6c pairwise contrasts effect estimate = -0.65, p = 0.37).

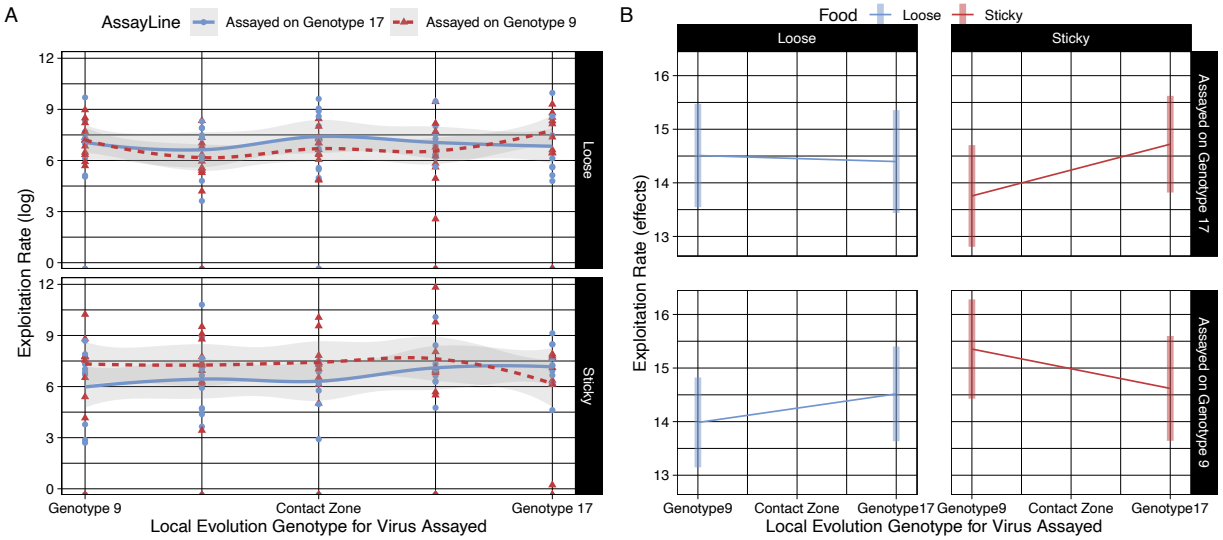

*Figure 4: Virus specialization within heterogeneous host populations depends on spatial structure. Virus sampled from different spatial positions within each microcosm (along x-axis with tick labels denoting the local evolution host genotype, i.e. Figure 1 vertical axes) were assayed on the two host genotypes. (A) Raw data for the composite exploitation rate (proportion infected * average number of occlusion bodies, log-scale, y-axis) on the two host genotypes (blue, circle, solid line is exploitation rate on genotype 17; red, triangle, dashed is on genotype 9) for virus from 'sticky' and 'loose' food microcosms (panels) for virus sampled from different spatial positions within the microcosm (x-axis) with therefore different evolutionary histories of mixing between the 2 host genotypes (B) Model effect estimates drawn from M6c GLMM for the interacting effects of food type and assay genotype on exploitation rate (y-axis) for virus sampled from different spatial positions within the microcosm with different degrees of mixing between the 2 host genotypes (x-axis). Panels are separated horizontally by food type and vertically by which host genotype the virus was assayed on.*

429 **DISCUSSION**

430 In our experiment, we find that pathogens can evolve to have higher exploitation rates on their
431 familiar host in spatially-structured microcosms and lower exploitation rates on their familiar
432 host in well-mixed microcosms. This effect holds at both the treatment level for virus lines
433 evolved in homogeneous host environments and as a gradient effect in heterogeneous host
434 environments where virus specializes on its locally familiar host (Figure 3, Figure 4). Therefore,
435 our experiment suggests that host genetic diversity and spatial structure interact to reverse the
436 outcome of specialization on pathogen exploitation rate.

437 However, the direction of these results is somewhat counterintuitive. These results would be
438 more simply explained if, in fact, well-mixed microcosms had higher exploitation rates on the
439 familiar host and spatially-structured microcosms had lower. This would match standard
440 expectations that virus in loose food (the more 'standard condition') should specialize on their
441 familiar host by increasing their exploitation rates, while virus in spatially structured conditions
442 may specialize on their familiar host by decreasing their exploitation rates (as in [30–32]) thereby
443 having higher exploitation rates on their foreign host. We saw the opposite.

444 Some theory suggests that intermediate spatial structure can actually select for higher parasite
445 exploitation rates under some conditions, however [28,33]. It is possible that our sticky food
446 microcosms fall into this region of the parameter space so that they were selected to have higher
447 exploitation rates on their familiar host. The fact that virus from well-mixed microcosms has
448 lower exploitation rates on the familiar host is harder to explain. The potential selection
449 pressures that we have measured (i.e. lower spatial structure, slightly faster development times)
450 should both select for increased exploitation of the familiar host. It is possible that there is a
451 phenotype under selection that we have not measured that negatively correlates with our
452 measured infectivity or productivity fitness metrics. The most likely candidate may be viruses'
453 time to kill (i.e. infection generation time) as virus could have a fitness benefit if they infect
454 multiple infection generations during our passages. Since our assays measure proportion infected
455 and virus productivity after a set period of time, we would not see this effect. In other baculovirus
456 systems, time to kill negatively correlates with virus productivity as virus can replicate more over
457 longer infection windows [62]. If this correlation holds in our system, selection for faster times
458 to kill would result in lower virus productivity, as in our results. It is even less clear why virus from
459 well-mixed conditions would have lower infectivity on their familiar host, but replication speed
460 in RNA viruses can also affect per particle infectivity so infectivity could also be potentially linked
461 to time to kill [63]. Our measured virus phenotypes could also be negatively correlated with other
462 unmeasured phenotypes like environmental decay [64] that could potentially explain these
463 results. Alternatively, virus from the 'loose' food condition may more closely approximate the
464 ancestral virus condition so that the selection for increased exploitation rate and higher force of
465 infection in 'sticky' food resulted in the faster evolution of higher familiar host exploitation, while
466 exploitation rates on foreign hosts drifted in different directions.

467 Another key, result of our experiment is that spatially structured heterogeneous host populations
468 support localized virus specialization and, therefore, more diverse viral strategies within the
469 population (Figure 4). Our experiment therefore supports theory suggesting that more contact
470 between host genotypes should select more strongly for generalism [20–22] and spatially

structured heterogeneity may support locally specialized virus populations [20]. Conceptually, this could mean that the benefits of genetic diversity in selecting for 'mediocre generalists' with constrained infectivity and virulence may be less realized when heterogeneity is spatially structured and can support assemblages of locally specialized pathogens. However, without knowing more about the phenotypes under selection in our experiment to understand which confer higher fitness, we cannot directly test this hypothesis.

Our results have implications for broader ecological and evolutionary theory on how specialization can support diversity. The fact that pathogens in our experiment can have (presumably) maladaptively high virulence on foreign hosts demonstrates that rare host genotypes may not always have a fitness advantage [65–68]. This has previously been considered in cases of species invasions (i.e. 'invading with weapons') and zoonosis [69,70], but not for host-parasite coevolutionary theory at equilibrium. The implications that certain spatial and population structures could systematically result in maladaptively higher exploitation rates on foreign, or rare, hosts could mean that they also vary in their likelihood to conform to the predictions of eco-evolutionary theory depending on rare genotype advantage like the Red Queen Hypothesis of Sex [71] and Janzen-Connell effects [72,73]. Additionally, our experiment shows that we should not always expect pathogens to have the highest exploitation rates on their familiar host, even in the absence of co-evolutionary dynamics where the host might be further 'ahead' in the arms race [74].

In this experiment, evolve granulosis virus in microcosms that vary in spatial structure and in the genetic diversity of the moth host to determine how these two selection pressures interact and how spatially structuring host heterogeneity affects parasite host range evolution. Our experiment shows that interactions between spatial structure and host genetic diversity alter the impact of specialization on pathogen evolution so that virus evolves higher exploitation rates on familiar hosts in well-mixed conditions and lower exploitation rates on familiar hosts in spatially structed conditions. We also see that spatially structured host heterogeneity can support local specialization. Our results suggest that there may be important interactions between parasite host range evolution and other selection pressures that could have implications for eco-evolutionary theory on the maintenance of diversity.

REFERENCES

1. King KC, Lively CM. 2012 Does genetic diversity limit disease spread in natural host populations? *Heredity* **109**, 199–203. (doi:10.1038/hdy.2012.33)

2. Gibson AK. 2022 Genetic diversity and disease: The past, present, and future of an old idea. *Evolution* **76**, 20–36. (doi:10.1111/evo.14395)

3. Zhu Y *et al.* 2000 Genetic diversity and disease control in rice. *Nature* **406**, 718–722. (doi:10.1038/35021046)

4. Elton CS. 1958 *The ecology of invasions by animals and plants.* Chicago, IL: University of Chicago Press. See https://www.cabdirect.org/cabdirect/abstract/19592202723.

510 5. Ekroth AKE, Rafaluk-Mohr C, King KC. 2019 Host genetic diversity limits parasite success
511 beyond agricultural systems: a meta-analysis. *Proc. R. Soc. B Biol. Sci.* **286**, 20191811.
512 (doi:10.1098/rspb.2019.1811)

513 6. Cornwall DH, Kubinak JL, Zachary E, Stark DL, Seipel D, Potts WK. 2018 Experimental
514 manipulation of population-level MHC diversity controls pathogen virulence evolution in
515 Mus musculus. *J. Evol. Biol.* **31**, 314–322. (doi:10.1111/jeb.13225)

516 7. White PS, Choi A, Pandey R, Menezes A, Penley M, Gibson AK, de Roode J, Morran L. 2020
517 Host heterogeneity mitigates virulence evolution. *Biol. Lett.* **16**, 20190744.
518 (doi:10.1098/rsbl.2019.0744)

519 8. Gibson AK, Nguyen AE. 2021 Does genetic diversity protect host populations from
520 parasites? A meta-analysis across natural and agricultural systems. *Evol. Lett.* **5**, 16–32.
521 (doi:10.1002/evl3.206)

522 9. Hughes WOH, Boomsma JJ. 2004 Genetic Diversity and Disease Resistance in Leaf-Cutting
523 Ant Societies. *Evolution* **58**, 1251–1260. (doi:10.1111/j.0014-3820.2004.tb01704.x)

524 10. González R, Butković A, Elena SF. 2019 Role of host genetic diversity for susceptibility-to-
525 infection in the evolution of virulence of a plant virus. *Virus Evol.* **5**.
526 (doi:10.1093/ve/vez024)

527 11. Kubinak JL, Ruff JS, Hyzer CW, Slev PR, Potts WK. 2012 Experimental viral evolution to
528 specific host MHC genotypes reveals fitness and virulence trade-offs in alternative MHC
529 types. *Proc. Natl. Acad. Sci.* **109**, 3422–3427. (doi:10.1073/pnas.1112633109)

530 12. Ekroth AKE, Gerth M, Stevens EJ, Ford SA, King KC. 2021 Host genotype and genetic
531 diversity shape the evolution of a novel bacterial infection. *ISME J.* **15**, 2146–2157.
532 (doi:10.1038/s41396-021-00911-3)

533 13. Levins R. 1962 Theory of Fitness in a Heterogeneous Environment. I. The Fitness Set and
534 Adaptive Function. *Am. Nat.* **96**, 361–373. (doi:10.1086/282245)

535 14. Fry JD. 1996 The Evolution of Host Specialization: Are Trade-Offs Overrated? *Am. Nat.* **148**,
536 S84–S107.

537 15. Whitlock MC. 1996 The Red Queen Beats the Jack-Of-All-Trades: The Limitations on the
538 Evolution of Phenotypic Plasticity and Niche Breadth. *Am. Nat.* **148**, S65–S77.

539 16. Regoes RR, Nowak MA, Bonhoeffer S. 2000 Evolution of Virulence in a Heterogeneous Host
540 Population. *Evolution* **54**, 64–71. (doi:10.1111/j.0014-3820.2000.tb00008.x)

541 17. Kawecki TJ. 1994 Accumulation of Deleterious Mutations and the Evolutionary Cost of Being
542 a Generalist. *Am. Nat.* **144**, 833–838.

543 18. Bono LM, Draghi JA, Turner PE. 2019 Evolvability Costs of Niche Expansion. *Trends Genet.* **0**.
544 (doi:10.1016/j.tig.2019.10.003)

545 19. Visher E, Boots M. 2020 The problem of mediocre generalists: population genetics and eco-
546 evolutionary perspectives on host breadth evolution in pathogens. *Proc. R. Soc. B Biol. Sci.*
547 **287**, 20201230. (doi:10.1098/rspb.2020.1230)

548 20. Gandon S, Poulin R. 2004 Evolution of multihost parasites. *Evolution* **58**, 455–469.
549 (doi:10.1554/03-390)

550 21. Osnas EE, Dobson AP. 2012 Evolution of Virulence in Heterogeneous Host Communities
551 Under Multiple Trade-Offs. *Evolution* **66**, 391–401. (doi:10.1111/j.1558-5646.2011.01461.x)

552 22. Williams PD. 2012 New Insights into Virulence Evolution in Multigroup Hosts. *Am. Nat.* **179**,
553 228–239. (doi:10.1086/663690)

554 23. Gandon S. 2002 Local adaptation and the geometry of host–parasite coevolution. *Ecol. Lett.*
555 **5**, 246–256. (doi:10.1046/j.1461-0248.2002.00305.x)

556 24. Gandon S, Capowiez Y, Dubois Y, Michalakis Y, Olivieri I. 1996 Local adaptation and gene-
557 for-gene coevolution in a metapopulation model. *Proc R Soc Lond B* **263**, 1003–1009.
558 (doi:10.1098/rspb.1996.0148)

559 25. Gandon S, Michalakis Y. 2002 Local adaptation, evolutionary potential and host–parasite
560 coevolution: interactions between migration, mutation, population size and generation
561 time. *J. Evol. Biol.* **15**, 451–462. (doi:10.1046/j.1420-9101.2002.00402.x)

562 26. Boots M, Sasaki A. 2000 The evolutionary dynamics of local infection and global
563 reproduction in host-parasite interactions. *Ecol. Lett.* **3**, 181–185.

564 27. Boots M, Sasaki A. 1999 'Small worlds' and the evolution of virulence: infection occurs
565 locally and at a distance. *Proc. R. Soc. B Biol. Sci.* **266**, 1933–1938.

566 28. Lion S, Boots M. 2010 Are parasites '"prudent"' in space? *Ecol. Lett.* **13**, 1245–1255.
567 (doi:10.1111/j.1461-0248.2010.01516.x)

568 29. Messinger SM, Ostling A. 2009 The Consequences of Spatial Structure for the Evolution of
569 Pathogen Transmission Rate and Virulence. *Am. Nat.* **174**, 441–454. (doi:10.1086/605375)

570 30. Boots M, Mealor M. 2007 Local Interactions Select for Lower Pathogen Infectivity. *Science*
571 **315**, 1284–1286. (doi:10.1126/science.1137126)

572 31. Kerr B, Neuhauser C, Bohannan BJM, Dean AM. 2006 Local migration promotes competitive
573 restraint in a host–pathogen 'tragedy of the commons'. *Nature* **442**, 75–78.
574 (doi:10.1038/nature04864)

575 32. Berngruber TW, Lion S, Gandon S. 2015 Spatial Structure, Transmission Modes and the
576 Evolution of Viral Exploitation Strategies. *PLOS Pathog.* **11**, e1004810.
577 (doi:10.1371/journal.ppat.1004810)

578 33. Kamo M, Sasaki A, Boots M. 2007 The role of trade-off shapes in the evolution of parasites
579 in spatial host populations: An approximate analytical approach. *J. Theor. Biol.* **244**, 588–
580 596. (doi:10.1016/j.jtbi.2006.08.013)

581 34. van Baalen M. 2002 Contact Networks and the Evolution of Virulence. In *Adaptive Dynamics*
582 *of Infectious Diseases: In Pursuit of Virulence Management*, Cambridge: Cambridge
583 University Press.

584 35. Amado A, Campos PRA. 2019 Ecological specialization under multidimensional trade-offs.
585 *Evol. Ecol.* **33**, 769–789. (doi:10.1007/s10682-019-10013-4)

586 36. Boots M, Childs D, Crossmore J, Tidbury H, Rudolf V. 2021 Experimental evidence that local
587 interactions select against selfish behaviour. *Ecol. Lett.* **24**, 1187–1192.
588 (doi:10.1111/ele.13734)

589 37. Boots M, Childs D, Reuman DC, Mealor M. 2009 Local Interactions Lead to Pathogen-Driven
590 Change to Host Population Dynamics. *Curr. Biol.* **19**, 1660–1664.
591 (doi:10.1016/j.cub.2009.07.070)

592 38. Visher E, Uricchio L, Bartlett L, DeNamur N, Yarcan A, Alhassani D, Boots M. 2022 The
593 evolution of host specialization in an insect pathogen. *Evolution* **76**, 2375–2388.
594 (doi:10.1111/evo.14594)

595 39. Stearns SC. 1989 Trade-Offs in Life-History Evolution. *Funct. Ecol.* **3**, 259–268.
596 (doi:10.2307/2389364)

597 40. Cressler CE, King AA, Werner EE. 2010 Interactions between Behavioral and Life-History
598 Trade-Offs in the Evolution of Integrated Predator-Defense Plasticity. *Am. Nat.* **176**, 276–
599 288. (doi:10.1086/655425)

600 41. Gage MJ. 1995 Continuous variation in reproductive strategy as an adaptive response to
601 population density in the moth Plodia interpunctella. *Proc. R. Soc. Lond. B Biol. Sci.* **261**, 25–
602 30. (doi:10.1098/rspb.1995.0112)

603 42. Mohandass S, Arthur FH, Zhu KY, Throne JE. 2007 Biology and management of Plodia
604 interpunctella (Lepidoptera: Pyralidae) in stored products. *J. Stored Prod. Res.* **43**, 302–311.
605 (doi:10.1016/j.jspr.2006.08.002)

606 43. Consigli RA, Tweeten KA, Anderson DK, Bulla LA. 1983 Granulosis Viruses, with Emphasis on
607 the Gv of the Indian Meal Moth, Plodia interpunctella. In *Advances in Virus Research* (eds
608 MA Lauffer, K Maramorosch), pp. 141–173. Academic Press. (doi:10.1016/S0065-
609 3527(08)60723-X)

610 44. Harrison RL, Rowley DL, Funk CJ. 2016 The Complete Genome Sequence of Plodia
611 Interpunctella Granulovirus: Evidence for Horizontal Gene Transfer and Discovery of an
612 Unusual Inhibitor-of-Apoptosis Gene. *PLoS ONE* **11**, e0160389.
613 (doi:10.1371/journal.pone.0160389)

614 45. Tidbury H. 2012 The Evolutionary Ecology of Antiviral Resistance in Insects. phd, University
615 of Sheffield. See http://etheses.whiterose.ac.uk/2937/.

616 46. Begon M, Daud KBH, Young P, Howells RE. 1993 The Invasion and Replication of a
617 Granulosis Virus in the Indian Meal Moth, Plodia interpunctella: An Electron Microscope
618 Study. *J. Invertebr. Pathol.* **61**, 281–295. (doi:10.1006/jipa.1993.1053)

619 47. Bartlett LJ, Wilfert L, Boots M. 2018 A genotypic trade-off between constitutive resistance
620 to viral infection and host growth rate. *Evolution* **72**, 2749–2757. (doi:10.1111/evo.13623)

621 48. Bartlett LJ, Visher E, Haro Y, Roberts KE, Boots M. 2020 The target of selection matters: An
622 established resistance—development-time negative genetic trade-off is not found when
623 selecting on development time. *J. Evol. Biol.* **33**, 1109–1119. (doi:10.1111/jeb.13639)

624 49. Oppert B, Hammel R, Throne JE, Kramer KJ. 2000 Fitness costs of resistance to Bacillus
625 thuringiensis in the Indianmeal moth, Plodia interpunctella. *Entomol. Exp. Appl.* **96**, 281–
626 287. (doi:10.1046/j.1570-7458.2000.00707.x)

627 50. Bolker BM, Brooks ME, Clark CJ, Geange SW, Poulsen JR, Stevens MHH, White J-SS. 2009
628 Generalized linear mixed models: a practical guide for ecology and evolution. *Trends Ecol.*
629 *Evol.* **24**, 127–135. (doi:10.1016/j.tree.2008.10.008)

630 51. R Core Team. 2021 *R: A language and environment for statistical computing.* Vienna,
631 Austria: R Foundation for Statistical Computing. See https://www.r-project.org/.

632 52. Bates D, Mächler M, Bolker B, Walker S. 2015 Fitting Linear Mixed-Effects Models Using
633 lme4. *J. Stat. Softw.* **67**, 1–48. (doi:10.18637/jss.v067.i01)

634 53. Brooks ME, Kristensen K, Benthem KJ van, Magnusson A, Berg CW, Nielsen A, Skaug HJ,
635 Mächler M, Bolker BM. 2017 glmmTMB Balances Speed and Flexibility Among Packages for
636 Zero-inflated Generalized Linear Mixed Modeling. *R J.* **9**, 378–400.

637 54. Fox J, Weisberg S. 2019 *An R Companion to Applied Regression, 3rd Edition*. See
638 https://socialsciences.mcmaster.ca/jfox/Books/Companion/index.html.

639 55. Hartig F, Lohse L. 2021 DHARMa: Residual Diagnostics for Hierarchical (Multi-Level / Mixed)
640 Regression Models.

641 56. Lenth RV, Buerkner P, Herve M, Love J, Miguez F, Riebl H, Singmann H. 2022 emmeans:
642 Estimated Marginal Means, aka Least-Squares Means.

57. Pedersen TL. 2020 patchwork: The Composer of Plots.

58. Singmann H *et al.* 2019 afex: Analysis of Factorial Experiments.

59. Wickham H. 2009 *ggplot2 - Elegant Graphics for Data Analysis*. Springer. See https://www.springer.com/gp/book/9780387981413.

60. Wickham H *et al.* 2019 Welcome to the Tidyverse. *J. Open Source Softw.* **4**, 1686. (doi:10.21105/joss.01686)

61. Harrison XA. 2014 Using observation-level random effects to model overdispersion in count data in ecology and evolution. *PeerJ* **2**, e616. (doi:10.7717/peerj.616)

62. Cooper V. S., Reiskind M. H., Miller J. A., Shelton K. A., Walther B. A., Elkinton J. S., Ewald P. W. 2002 Timing of transmission and the evolution of virulence of an insect virus. *Proc. R. Soc. Lond. B Biol. Sci.* **269**, 1161–1165. (doi:10.1098/rspb.2002.1976)

63. Fitzsimmons WJ, Woods RJ, McCrone JT, Woodman A, Arnold JJ, Yennawar M, Evans R, Cameron CE, Lauring AS. 2018 A speed–fidelity trade-off determines the mutation rate and virulence of an RNA virus. *PLOS Biol.* **16**, e2006459. (doi:10.1371/journal.pbio.2006459)

64. Ogbunugafor CB, Alto BW, Overton TM, Bhushan A, Morales NM, Turner PE. 2013 Evolution of Increased Survival in RNA Viruses Specialized on Cancer-Derived Cells. *Am. Nat.* **181**, 585–595. (doi:10.1086/670052)

65. Abrams PA. 2006 The Prerequisites for and Likelihood of Generalist-Specialist Coexistence. *Am. Nat.* **167**, 329–342. (doi:10.1086/499382)

66. Chesson P. 2000 Mechanisms of Maintenance of Species Diversity. *Annu. Rev. Ecol. Syst.* **31**, 343–366. (doi:10.1146/annurev.ecolsys.31.1.343)

67. Gibson AK, White PS, Penley MJ, de Roode JC, Morran LT. 2020 An experimental test of parasite adaptation to common versus rare host genotypes. *Biol. Lett.* **16**, 20200210. (doi:10.1098/rsbl.2020.0210)

68. Lively CM, Dybdahl MF. 2000 Parasite adaptation to locally common host genotypes. *Nature* **405**, 679. (doi:10.1038/35015069)

69. Guth S, Mollentze N, Renault K, Streicker DG, Visher E, Boots M, Brook CE. 2022 Bats host the most virulent—but not the most dangerous—zoonotic viruses. *Proc. Natl. Acad. Sci.* **119**, e2113628119. (doi:10.1073/pnas.2113628119)

70. Tompkins DM, White AR, Boots M. 2003 Ecological replacement of native red squirrels by invasive greys driven by disease. *Ecol. Lett.* **6**, 189–196. (doi:10.1046/j.1461-0248.2003.00417.x)

71. Jaenike J. 1978 A hypothesis to account for the maintenance of sex within populations. *Evol Theory* **3**, 191–194.

72. Connell JH. 1971 On the role of natural enemies in preventing competitive exclusion in some marine animals and in rain forest trees. *Dyn. Popul.* **298**, 312.

73. Janzen DH. 1970 Herbivores and the Number of Tree Species in Tropical Forests. *Am. Nat.* **104**, 501–528. (doi:10.1086/282687)

74. Greischar MA, Koskella B. 2007 A synthesis of experimental work on parasite local adaptation. *Ecol. Lett.* **10**, 418–434. (doi:10.1111/j.1461-0248.2007.01028.x)